Filtration of Liquid Aerosols on Nonwettable Fibrous Filters

Igor E. Agranovski and Roger D. Braddock
Environmental Sciences, Griffith University, Nathan, Australia 4111

Chemical, manufacturing and refining processes often generate toxic liquid by products that are emitted as liquid aerosols in the waste stream. Wettable and nonwettable fibers can be used to filter these exhaust streams. The behavior of liquid aerosols and droplets on nonwettable fibers is studied by observation, measurement, and theory. Droplets form on the fibers, grow by accretion from the aerosol, oscillate, and then fall under the action of gravity. Observation and theory indicate that these developing droplets influence air and aerosol flow strongly in the filter. These droplets are akin to the dendritic structures formed by solid aerosol particles within filters, but the shapes are modified by surface tension. The total efficiency of the filter is influenced by these droplets, and the total filter efficiencies are estimated using theoretical methods. The results from both approaches agree excellently in the particle-size range as measured using particle-counting techniques.

Introduction

Filtration processes and systems are used to control and regulate the concentration of waste products in the exhaust streams from industrial, chemical, and mining operations. Filter operation has long been the subject of research, both experimental and theoretical, and Davies (1973) provides an overview of the subject. Classical filtration theory can be applied to fresh or clean filters to estimate the particle separation efficiency, and other flow characteristics (Hinds, 1982; Brown, 1993). The classical theories are usually no longer applicable to dirty filters which carry deposits on the fibers. These deposits may alter the flow characteristics in the filter, considerably altering the filtering properties. Sometimes, and especially for highly concentrated gas streams, the variations to the flow field are so significant that the filter plants operate poorly and nowhere near the original design criteria. This clogging of the filters can result in frequent and costly cleaning and maintenance operations.

The filtration of liquid particles from exhaust streams is particularly important in the chemical industry where the waste liquid aerosols may be highly toxic or corrosive, such as the manufacture of sulfuric acid. In such cases, it may be possible to design a self-cleaning filter whereby the liquid particles collect on the filter and then drain down to some collecting device. Such a self-cleaning filter can remain operational and near its design specifications for an almost indefinite period. Operational and maintenance costs are substantially reduced.

The filtration of liquid aerosols by fiber filters has received little attention in the literature. Fairs (1958) described the mechanisms operating in the filtration of fine mists, and also considered the high efficiencies which could be obtained. Eriksson et al. (1992) also investigated the adhesion forces between the fibers as a result of condensation of an aerosol on the filter. Payet et al. (1990) experimented with glass fiber filters and submicrometer oil on the fibers. They found that the amount of oil on the filter affected the measured pressure drop across the filter. Agranovski (1995) identified the influence of wettability/nonwettability between aerosol and fiber on the efficiency of filtration. Agranovski also identified the forces acting, and provided some simple and practical models of the flow fields. Agranovski and Braddock (1998) investigated the theoretical and experimental efficiencies of a wettable filter and aerosol.

Various parameters of the filter and the exhaust stream need to be considered. These include the physical and chemi-

Correspondence concerning this article should be addressed to I. E. Agranovski.

cal properties of the waste liquid and the physical properties of the carrier gas such as temperature, velocity, and moisture content. However, the wettability/nonwettability of the filter fibers in relation to the liquid aerosol is one of the most important parameters of liquid aerosol filtration (Agranovski, 1995). It has been shown that liquid aerosols will adhere to wettable filter fibers and form liquid films about the fibers (Agranovski, 1995; Agranovski and Braddock, 1998). These films form drainage paths down the filter fibers and provide a self-cleaning mechanism. However, liquid aerosol particles are not spread along nonwettable fibers, although the filter intercepts their path. These nonwettable fibers can force the liquid particles to form droplets on the fibers, and these droplets then drain from the filter to a collection device at the bottom.

The objectives of this article are to investigate the nature of liquid aerosol on the filtration process, as affected by the nonwettable fibers in the filter, and to assess the effects on the filtration efficiencies. Observations of the relevant processes are made and measurements are reported on the structure of the self-draining properties of the nonwettable fibers. Models of the filtration efficiency are constructed and compared with observations.

Experimental Plant and Preliminary Observations

The experimental program required the design and construction of a suitable laboratory plant. A brief description of the plant is given in Agranovski and Braddock (1998) and details of the design and instrumentation are given in Agranovski (1995). The observations and experimental work were performed with filters manufactured from teflon and polypropylene which are not wettable by water which was used in the experiments. The filter and fiber parameters are given in Table 1. For each material, the filters were 1 m in height, 30 cm in width, and the corresponding thicknesses are given in Table 1.

Some preliminary observations were carried out using the observation window in the filter box. The objective was to gain an initial understanding of the filtration processes, to observe the interaction between the aerosol and the fibers, and to provide guidance for the more precise theoretical and experimental work. These observations were conducted with an air flow of 1 m/s, 85% humidity, 20°C, and with a water aerosol concentration of 3 g/m^3. The filters were dry when inserted into the filter box; then, the plant was activated.

Observation of the filter indicated that the aerosol particles hit the filter and adhere mainly to its surface. These droplets on the filter do not spread out along the fibers (as was observed for wettable fibers by Agranovski and Braddock, 1998), but remain as spheres. These spherical droplets

Table 1. Properties of Nonwettable Fibers and Filters Used in Experiments

Material	Dia.	Packing Dens.	Thickness
Teflon	27 μm	4%	7 mm
Polypropylene	19 μm	3%	6 mm

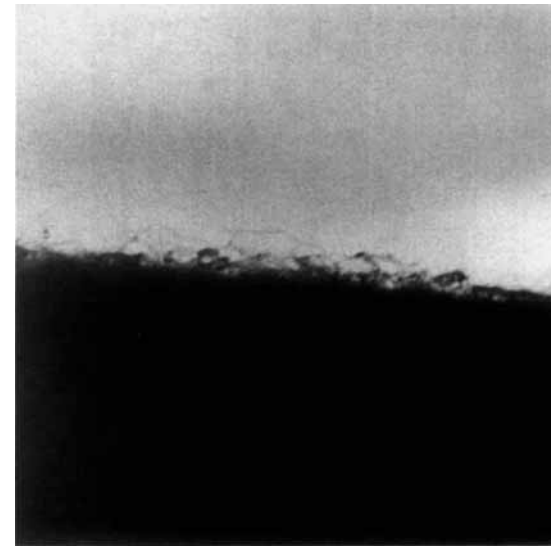

Figure 1. Droplets on the surface of the nonwettable (teflon) filter.

grow by accretion with incoming aerosol particles. As the droplet grows, it reaches a certain critical limit, begins to oscillate, and then detaches and falls down the filter. During this stage, the force of gravity on the droplet overcomes the adhesion forces between the droplet and the fibers, causing the droplet to fall. Generally, the fan and aerosol need to operate for at least 30 min for the process to stabilize or reach the equilibrium state. It was also noted that the droplets were uniformly distributed across the face of the filter.

Unfortunately, the optical properties of water are very similar to those of teflon, polypropylene, and the other common nonwettable fibers, and it is difficult to get sufficient contrast to obtain clear photographs of the filter *in situ*. However, once the equilibrium state had been reached, the filter was removed from the filter box, carefully bent, and the surface of the filter was photographed. One such photograph is shown in Figure 1; it shows liquid spheres resting on the surface of the teflon filter. There is little other detail visible in the image.

A further experiment was conducted by fixing a single teflon fiber in a specially designed holder, and placing this in a sealable chamber. Some water was placed on the bottom of the chamber to ensure 100% humidity. Water droplets were then supplied from an atomizer. After two droplets had formed on the single fiber, the chamber was hermetically sealed, and the droplets were observed at regular intervals over a period of 3 h. Figure 2a shows the fiber and the freshly formed droplets on installation in the sealed chamber. In the sealed chamber, the droplets did not change position, shape or size over the 3-h period of observation. The droplets did not wet the teflon and did not form a film over the surface of the fiber, as observed by Agranovski and Braddock (1998) for the wettable fiber case. Obviously, the droplets were small enough for the adhesion forces to overcome the force of gravity.

After 3 h in the chamber, the fiber and droplets were removed from the chamber and mounted in the open room. Figure 2b shows the droplets 7 min after opening the cham-

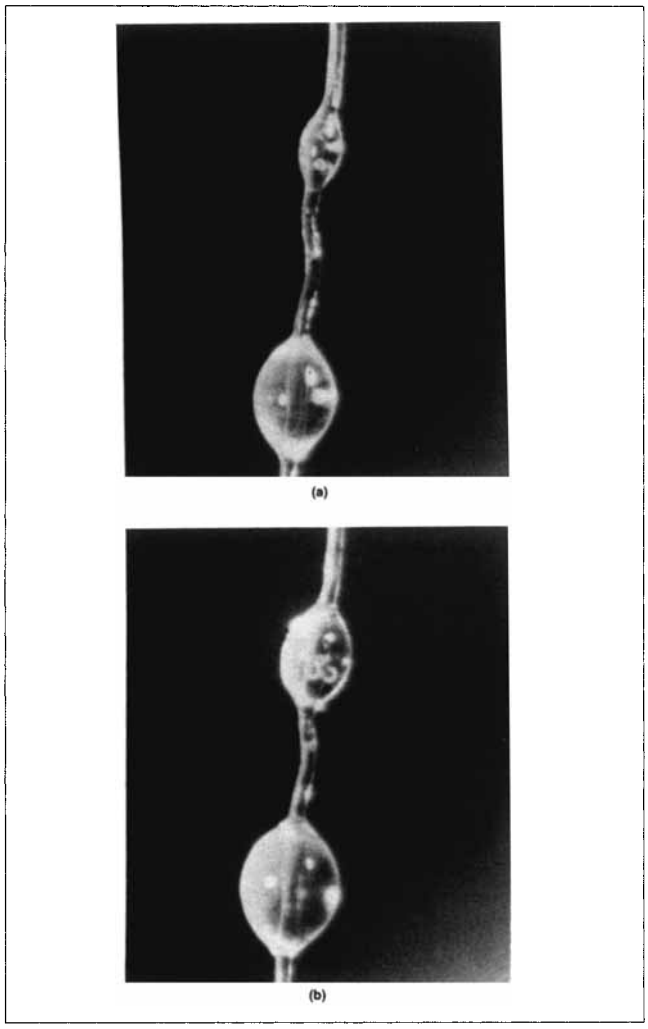

Figure 2. Droplets on the single teflon fiber.

(a) In the sealed chamber immediately after installation (100%) relative humidity; (b) removed from the sealed chamber 7 min after being located in the open air.

ber. The diameter of the drops is decreasing as the droplets evaporate in the drier air.

The first set of observations dealt with water droplets accumulating on the front face of the filter, and these could be photographed with special techniques. The presence of droplets inside the filter was also observed, but these could not be photographed *in situ*. Some observations were made by running the filter plant to equilibrium, turning it off, removing the wet filter, and then carefully separating the filter into layers to expose the internal droplets. Given the physical handling which was required, the validity of the observations is not strong. However, generally there were many more droplets on the face of the filter than in the interior and the droplets on the face were large.

Theoretical Aspects

The droplets which adhere to the filter fibers block the flow of gas and alter the effective packing density of the filter. The effective packing density of the filter can be determined by theory and experimental measurement.

Consider the one-dimensional flow of dry air across the filter. Then, the volume flux is given by $A_d U_d$, where A_d is the effective area of the filter transmitting the air and U_d is the face velocity of the dry air. This volume flux is provided principally by a fan. The total volume flux from the fan remains the same when the filter is wet and at equilibrium. Then, the equation of continuity yields

$$A_d U_d = (A_d - A_b) U_w, \tag{1}$$

where U_w is the face velocity of the wet airstream at equilibrium and A_b is the area of the filter occupied by suspended drops.

Now consider a droplet suspended on the surface of, or inside, the filter material. Assume that each droplet of diameter D_d is located in a cubic cell, as shown in Figure 3. The edge length of the cell is XD_d, where X is a scale factor and the cell is oriented with one face parallel to the forward face of the filter.

The ratio of the projected area of the sphere $S_d = \pi(D_d/2)^2$ to the area of the forward face of the cell is a measure of the blocking of the air flow by the droplet. The size of the cell is selected by equating this ratio with the ratio of the blocked area (of the filter) to the area of the filter A_f or

$$\frac{\pi D_d^2}{(D_d X)^2} = \frac{A_b}{A_f} \tag{2}$$

For the cell in Figure 3, but ignoring the droplet, the theoretical packing density c_T of the filter is given by

$$c_T = \pi \left(\frac{d_f}{2}\right)^2 \frac{L_f}{(D_d X)^3}, \tag{3}$$

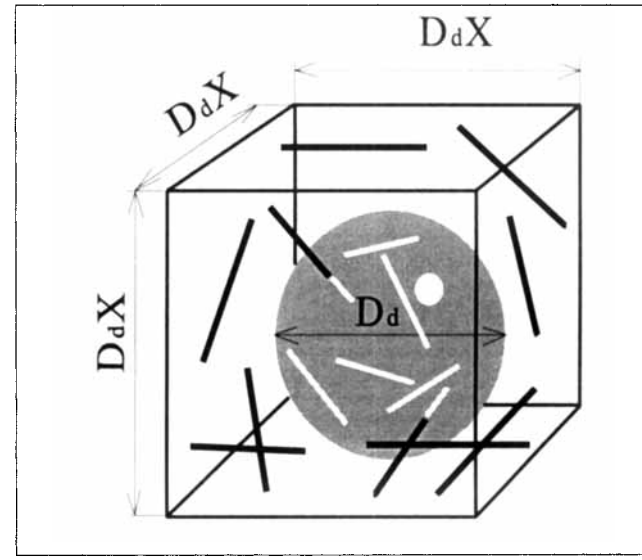

Figure 3. Conceptual droplet and cubic cell.

where d_f is the diameter of the fiber, L_f is the total length of the fiber in the cell, and x is given by Eq. 4. The total forward-facing, cross-sectional area S_c of fibers in the cell is given by

$$S_c = d_f L_f, \tag{4}$$

and on substituting for L_f using Eq. 4

$$S_c = 4(D_d X)^3 \frac{c_T}{\pi d_f}. \tag{5}$$

Now consider the cell and the droplet and let L_{fd} be the length of the fiber in the droplet. The volume of fiber in the droplet is given by

$$L_{fd}\pi\left(\frac{d_f}{2}\right)^2 = c_f \times \frac{4}{3}\pi\left(\frac{D_d}{2}\right)^3, \tag{6}$$

where the righthand side is the packing density multiplied by the volume of the droplet. Then the frontal area S_{fd} of the fiber in the droplet is

$$\begin{aligned} S_{fd} &= d_f L_{fd} \\ &= 2D_d^3 \frac{c_T}{3d_f}. \end{aligned} \tag{7}$$

Then the equivalent frontal area S_c of the filter in each cell is

$$\begin{aligned} S_e &= S_c + S_d - S_{fd} \\ &= \frac{4X^3 D_d^3 c_T}{\pi d_f} + \frac{\pi D_d^2}{4} - \frac{2D_d^3 c_T}{3d_f}. \end{aligned} \tag{8}$$

Now the effective packing density c_e of the cell is given by

$$c_e = \frac{4X^3 D_d c_T + 0.785\pi d_f - 0.66\pi D_d c_T}{4X^3 D_d}. \tag{9}$$

Using the classical theory of filtration, the single-fiber efficiency η can be calculated as the arithmetic sum

$$\eta = \eta_i + \eta_R + \eta_D + \eta_{DR}, \tag{10}$$

where η_i, η_D, and η_R are the single-fiber efficiencies of inertia, diffusion, and interception, and η_{DR} is the single-fiber efficiency of the diffusion-interception interaction. Suitable formulae for the estimation of these efficiencies are given by Hinds (1982). The theoretical efficiency of the filter E_T may then be estimated from (Hinds, 1982)

$$E_T = 1 - \exp\left[\frac{-4\eta c_e H}{\pi d_f}\right], \tag{11}$$

where d_f is the diameter of fiber, and H is the thickness of the filter.

Experimental Studies

An experimental program was carried out to investigate the properties of the droplets on the filter, and to assess their effects on the efficiency of the filter.

Behavior of droplets

The growth and detachment of the droplets on the front surface of the filter were measured using a cathetometer, a device to measure the distance between the top and bottom of the droplet. The plant was then run for face velocities of 0.5 (0.25) 4 m/s, and the diameter of the droplet, just before it fell, was recorded.

It was not possible to measure directly the size of the droplet inside the filter while the plant was running. However, when the runs were finished, the filters were removed, separated into layers, and measurements of the diameters of internal droplets were taken.

Pressure drop and effective packing density

The blocking of the filter by droplets will affect the resistance of the filter and the gas-flow field. Given the observation that the droplets are uniformly distributed, there is no flow or resistance variations down the filter. A U-tube manometer was installed to measure the pressure drop of the gas flow across the filter. In each experimental run, the filter was installed dry, the air flow was started, and the pressure drop was measured. Then, the aerosol generator was turned on and the filter was allowed to become wet and to attain a steady operating state. As the filter becomes wetter, the pressure drop increases and then stabilizes at the operating level. The final pressure drops were then taken and recorded as a function of face velocity and of aerosol concentrations. Face velocities ranged from 0.5 to 5 m/s, and the aerosol concentrations of 0 (dry), 0.5, 1.0 and 5.0 g/m^3 were used. Obviously, the time to reach the equilibrium condition depended inversely on the aerosol concentration. Experiments were performed for both teflon and polypropylene filters.

Efficiency of filtration

The experimental efficiency of a filter is given by (Hinds, 1982)

$$E_E = 1 - \frac{\text{final aerosol concentration}}{\text{initial aerosol concentration}} \tag{12}$$

and this may be evaluated by direct measurement of the initial and final aerosol concentrations. Aerosol concentrations were measured using a Malvern particle-size analyzer (detection range 0.5 to 650 μm) in combination with a particle counter and the cascade impactor (detection range 0.2 to 20 μm). Measured efficiencies were obtained for the size range 0.5 to 20 μm, the range which is common to both techniques. The experiments were carried out for aerosol sizes in this

range, and a gas face velocity of 1 m/s, the speed usually employed in industrial applications.

Results and Discussion

The experimental results reveal some of the properties of the droplets and their effect on the filtration efficiency.

Behavior of droplets

Figure 4 shows the results of the average droplet size at detachment as a function of face velocity. Approximately ten observations were made at each velocity, and the results were averaged; the variation in size across the experiments for each velocity category was not large. STDEV did not exceed 0.17.

Obviously, the maximum diameter varies with the face velocity and decreases as the face velocity increases with dramatic change in the velocity range 1.5 to 2.75 m/s. It was also observed that, as the diameter increased toward (and near) the maximum, the droplet began to oscillate. On reaching the maximum diameter, the oscillations grew in amplitude and the droplet fell from the filter. This phenomenon was not apparent at velocities below 1.0 m/s. This phenomenon seems to be a response to a transition from laminar to turbulent flow of the air around the droplet.

The Reynolds number Re for flow around the sphere is

$$Re = \frac{U_w D_d \rho_g}{\mu_g}, \tag{13}$$

where U_w is the face velocity of the gas, ρ_g is the gas density, and μ_g is its viscosity.

Valdberg et al. (1993) suggest that the turbulent transition occurs for $Re \approx 150$, for which

$$U_w = 2.25 \times 10^{-3} \times D_d^{-1}, \tag{14}$$

on substituting in Eq. 13. This curve is shown on Figure 4, separating the laminar and turbulent regimes. This figure shows good agreement between the two curves for $U_w \geq 1.5$ m/s.

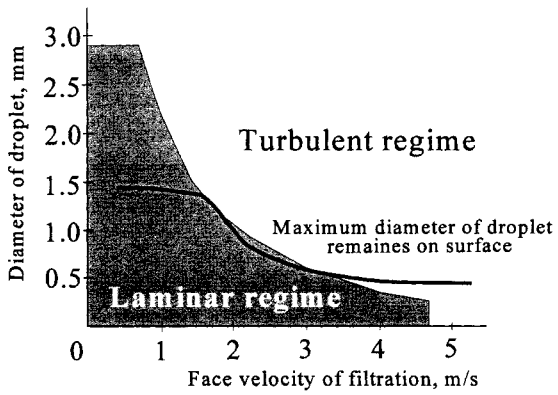

Figure 4. Maximum diameter of droplet on filter surface as a function of face velocity, and the laminar/turbulent regimes.

There is a major divergence of the curves for U_w below 1.5 m/s. In this region, gravity effects become important before the onset of turbulence and the gravity forces overcome the adhesion forces. The droplets fall by accretion and gravity before the onset of the laminar/turbulent transition.

As the face velocity is increased, the droplets grow by accretion into the transition region, and the drag forces on the droplet become significant compared to gravitational forces. A possible explanation is that the gas flow around the drop may become oscillatory in nature in a 3-D analog of the 2-D Karman vortex sheet (Lamb, 1945). Then a complex oscillatory interaction may occur between the droplet and the flow field, and the droplet falls from the filter.

For face velocities above about 3.3 m/s, the flow is more turbulent, with a less oscillatory component. Here, oscillatory forces in the vertical direction are less, and the adhesion forces can hold the droplet on the filter for longer. Thus, the diameter of the droplet needs to grow to the stage where turbulent drag and gravity is sufficiently large to overcome the adhesion.

It was also observed that the droplets grew almost linearly in time. Now the droplet of diameter D_d grows in volume v_d by accretion of aerosol particles to its frontal surface area. Thus,

$$\frac{dv_d}{dt} = q\pi\left(\frac{D_d}{2}\right)^2. \tag{15}$$

where the constant of proportionality q depends on the flux of aerosol (assumed constant). Now

$$v_d = \frac{4\pi}{3}\left(\frac{D_d}{2}\right)^3, \tag{16}$$

and hence dD_d/dt is constant. Thus, D_d is a linear function of time, as observed in the experiments.

Some observations were made of the droplet sizes inside the filter. Generally, these droplets had diameters below 0.4 mm, which is generally smaller than those on the front face of the filter. The front face is capturing a major part of the aerosol, and only a fraction is penetrating the filter. The internal droplets also suffer more evaporation from their surface, as they take longer to grow and are located in a less concentrated air stream. The process of stripping apart the filter may also cause errors in the measurements.

Pressure drop and packing density

The measured pressure drops for teflon (Figure 5a) and polypropylene (Figure 5b) exhibit a strongly linear relationship to the face velocities. In each case, the pressure drop is not markedly altered by the aerosol concentration, although the larger diameter teflon has produced a steeper slope in the pressure drop. This linearity implies that

$$\Delta P = b_1 U, \tag{17}$$

where ΔP and U refer to either wet or dry filters, and b_1 is a constant of proportionality. Thus, the ratio U_d/U_w of face ve-

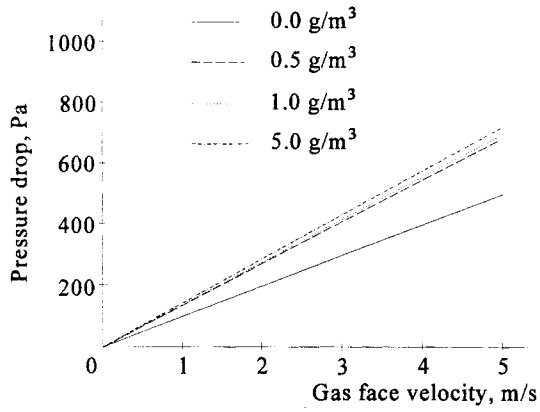

Figure 5a. Pressure drop across the teflon filter.

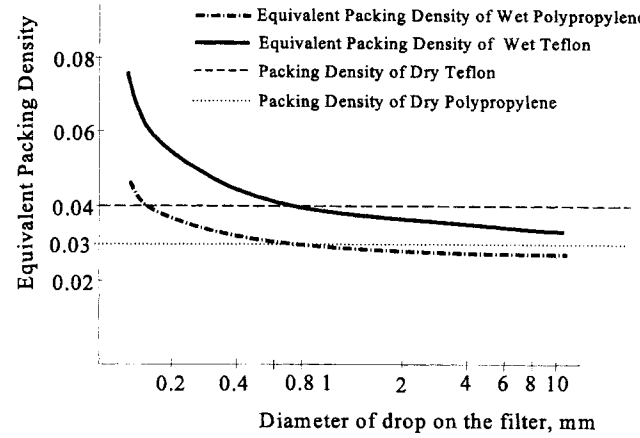

Figure 6. Equivalent packing densities for teflon and polypropylene as a function of droplet diameter.

locities in Eq. 2 can be replaced by the ratio ΔP (dry)/ΔP (wet) and the blocked area of the filter can be estimated. Thus, for teflon, 29% of the filter is blocked by water droplets, while for polypropylene, the percentage blocked is 21%. Using Eq. 3, then $X_{\text{teflon}} = 1.65$, and $X_{\text{polypropylene}} = 1.93$.

Then, Eq. 9 can be used to estimate the equivalent packing densities for the two filters and the results are shown in Figure 6, where the packing densities are shown as a function of the droplet diameter D_d. For teflon, the effective packing density is larger than the dry packing density of 4% (see Table 1) for $D_d < 0.8$ mm; for polypropylene, the corresponding cross-over point is at $D_p < 0.75$ mm. When the droplet sizes are larger than these respective values, it means that the frontal area of the fibers located within a droplet are larger than the frontal area of the droplet itself.

Efficiency of filtration

Figure 7 (teflon) and Figure 8 (polypropylene) show the measured filtration efficiencies using the Malvern and Cascade Impactor instruments for a range of particle diameters. The measured aerosol particle concentrations were converted to efficiencies using Eq. 12. Both figures show little variation between the efficiencies as measured by both instruments; that is, the error is less than 6%. For particle diameters above 4 μm, the efficiencies are close to 100%. Below 4 μm, the efficiency drops to a minimum of 25% at particle diameters of the order of 0.9 μm for teflon, and 35% at the same particle diameter for polypropylene. The efficiency then starts to rise for smaller particle diameters down to the limit of detectability of the instruments.

Theoretical estimates of the efficiency of filtration were also made using Eqs. 10 and 11, and the appropriate formulae from Hinds (1982). These formulae require estimates of the effective packing density and other parameters of the flow field. Note that Figures 4 and 6 provide relations between the effective packing density c_e, the maximum droplet diameter D_d and the face velocity. Theoretical estimates of the filtration efficiency were calculated for teflon fibers using the effective packing densities of 0.0379, 0.04, 0.0407 and 0.0538. These were selected on the basis of

(a) $c_e = 0.0379$ corresponds to a maximum droplet diameter of 1.4 mm for a face velocity of 1 m/s (see Figures 4 and 6).

(b) $c_e = 0.0407$. The diameters of the drops grow linearly in time (see Eq. 15 and the subsequent discussion), and a

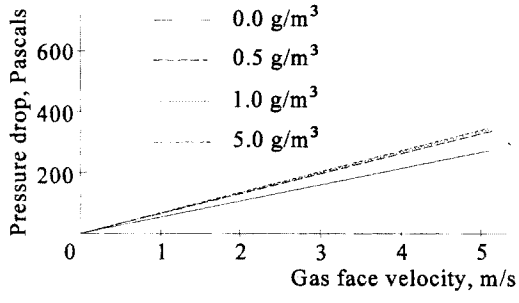

Figure 5b. Pressure drop across the polypropylene filter.

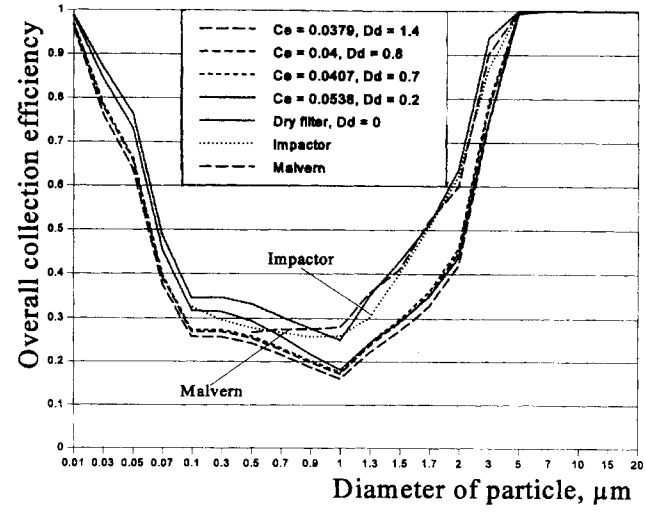

Figure 7. Experimental and theoretical efficiencies for the teflon filter.

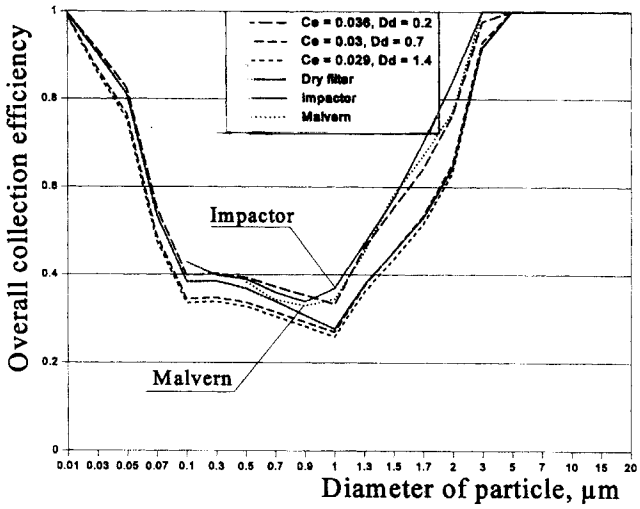

Figure 8. Experimental and theoretical efficiencies for the polypropylene filter.

diameter of 0.7 mm is half of the maximum obtained for a face velocity of 1 m/s. This packing density corresponds to the average droplet diameter on the filter.

(c) $c_e = 0.04$ corresponds to the droplet diameter of 0.8 mm at the cross-over point on Figure 6; again with a face velocity of 1 m/s.

(d) $c_e = 0.0538$. The largest drops inside the filter had a diameter of 0.4 mm. This packing density corresponds to the average diameter of 0.2 mm.

The results of the theoretical calculations for a dry teflon filter and a wet filter with the above packing densities are shown in Figure 7. Similar theoretical estimates of the filter efficiency for polypropylene were undertaken for the effective packing densities 0.029, 0.3, and 0.036. The choice of 0.03 corresponds to the polypropylene cross-over point in Figure 6 and corresponds to item (c) above.

The results for the theoretical efficiencies for polypropylene are shown in Figure 8. The results for the dry filter and for the lower packing densities for teflon (Figure 7) underestimate the measured efficiency of filtration with a maximum error of some 20%. However, the theoretical result for $c_e = 0.0538$ is very close to the measured values, with a maximum error of about 5%, and that at the lower limits of detection by the instruments.

The results and comparison with experiments for polypropylene (Figure 8) follow a similar pattern. The theoretical results for the dry filter and smaller packing densities give low estimates of the filtration efficiencies with errors up to 15%. However, the theoretical result for $c_e = 0.036$ compares very well with the experimental results.

Conclusions

The filtration of liquid aerosols by nonwettable fiber filters was studied by a mixture of observation, theoretical, and experimental techniques. Observations indicate that the liquid forms droplets on the face and interior of the filter, and that these grow in time. Depending on the experimental parameters, these droplets reach a critical size at which they begin to oscillate, then break free and fall from the filter. This provides a self-draining/cleaning mechanism for the filter.

The size of the droplets affects the pressure drop across the filter and influences its efficiency. The effective packing density of the filter can be estimated using simple models of the surface of the filter. The results can be used to estimate the theoretical efficiency of filtration, and these can be compared with the experimental results for the measured efficiencies. The lower estimates of the packing density underestimate the measured efficiencies by up to 20%. However, the large values of c_e provide good agreement of the theoretical and measured efficiencies. Both results show relatively poor filtration efficiencies for the aerosol size range of 0.1 to 1.5 μm.

The self-cleaning nature of the nonwettable filter has important applications in industry for the filtering of liquid aerosols. The draining droplets are readily collected at the base of the filter and can be led away for further processing or returned to an earlier stage of the industrial operation.

Literature Cited

Agranovski, I. E., "Filtration of Ultra-Small Particles on Fibrous Filters," PhD Thesis, Griffith University, Nathan, Australia (1995).

Agranovski, I. E., and R. D. Braddock, "Filtration of Liquid Aerosols on Wettable Fibrous Filters," *AIChE J.*, in press (1998).

Brown, R. C., *Air Pollution: An Integrated Approach to the Theory and Applications of Fibrous Filters*, Pergamon Press, Oxford (1993).

Davies, C. N., *Air Filtration*, Academic Press, London (1973).

Eriksson, J., S. Ljunggren, and L. Ödberg, "Adhesive Forces Between Fibres due to Capillary Condensation of Water Vapour," *J. Coll. Int. Sci.*, **152**(2), 368 (1992).

Fairs, G., "High Efficiency Fibre Filters for the Treatment of Fine Mists," *Trans. Inst. Chem. Engrs.*, **36**, 476 (1958).

Hinds, W. C., *Aerosol Technology*, Wiley, New York (1982).

Lamb, H., *Hydrodynamics*, Dover Press, New York (1945).

Payet, S., P. Bouland, G. Madeleine, and A. Renoux, "Dynamic Filtration of Liquid Aerosols," *Proc. of World Filtration Cong.*, 617 (1990).

Valdberg, A. J., L. M. Isianov, and J. I. Iadamov, *Theoretical Foundations of Environmental Protection from Particulate Pollutants* (in Russian), Niiogas-Filter, St. Petersburg, Russia (1993).

Manuscript received Mar. 30, 1998, and revision received Sept. 8, 1998.